Primer on the Estimation of Sea Surface Temperature Using TeraScan Processing of NOAA AVHRR Satellite Data
Version 2.0
S1R–96M–03

Frank Monaldo
The Johns Hopkins University
Applied Physics Laboratory

October 22, 1997

Contents

Abstract

In this memorandum, we review the physics of blackbody radiation and its application to the determination of sea surface temperature using infrared measurements. We describe the process of using infrared measurements at various wavelengths to correct for the interference of the atmosphere in estimating sea surface temperature from spaceborne instruments. Finally, we outline the standard steps used by the TeraScan software from SeaSpace Corporation to convert infrared radiance measurements to sea surface temperatures.

1   Introduction

Infrared radiance measurements have been used since 1970 to estimate sea surface temperature from space. The techniques for estimating sea surface temperature are based on the physics of blackbody radiation. Solutions are also required to practical problems such as correcting for the effects of the intervening atmosphere, identifying cloud-free regions, and navigating the measurements to ground coordinates.

The National Oceanic and Atmospheric Administration (NOAA) currently uses two polar-orbiting satellites, NOAA-12 and NOAA-14, for twice-daily global observations of sea surface temperature. These satellites are equipped with the Advanced Very High Resolution Radiometer (AVHRR) which scans the surface with a nadir resolution of 1.1 km and continuously broadcasts the data to ground receiving stations within the line of sight.

The Space Oceanography Group at the Johns Hopkins University Applied Physics Laboratory (JHU/APL) has recently implemented a capability to receive, process, and archive AVHRR data using the JHU/APL Satellite Communications Facility and hardware/software purchased from SeaSpace Corporation. This memo:

1. Reviews the pertinent physics of blackbody radiation,

2. Describes the algorithms used to derive sea surface temperatures from multiple-wavelength infrared measurements, and

3. Outlines the procedures used by the SeaSpace TeraScan software to produce sea surface temperature estimates.

2   Physics

2.1   BlackBody Radiation

By virtue of molecular motion, all substances above absolute zero emit radiation. A body that absorbs all incoming radiation is referred to as a *blackbody* [1] [2]. The wavelength distribution of the radiation from a blackbody, $B(\lambda, T)$, was measured in the last century. In 1893, Wien derived the following functional form for this distribution:

$$B(\lambda, T) = \frac{f(\lambda T)}{\lambda^5} \tag{1}$$

where λ is electromagnetic wavelength, T is absolute temperature and $f(\lambda T)$ is a function of the product of wavelength and temperature. This distribution function fit the observed data which showed that the radiation went to zero at the extremes of short and long wavelengths.

Using classical electromagnetic theory, Raleigh and Jeans predicted that at short wavelengths the emitted energy should grow to infinity, in contradiction to the observed data. This lack of correspondence between observation and the theoretical prediction of classical electromagnetics was known as the Raleigh-Jeans catastrophe.

In 1901, Planck made the simple assumption that energy can only exist in discrete packets or quanta. The energy is these packets equals $h\nu$ where h is Planck's constant and ν is the electromagnetic frequency. From this and thermodynamic considerations, Planck derived the blackbody spectral radiance as

$$B(\lambda, T) = \frac{2hc^2}{\lambda^5} \frac{1}{\exp[hc/(kT\lambda)] - 1} \tag{2}$$

where c is the speed of light and k is Boltzmann's constant.

Real objects are not perfectly absorbing and hence they emit less radiation than predicted by this equation. The emissivity of a real object $\varepsilon(\lambda, T)$ is defined as the ratio of the amount of radiation emitted by the object to that of a blackbody at the same temperature and wavelength. Note that $\varepsilon \leq 1$.

2.2   Estimation of Temperature

A radiometer measures radiation over a finite wavelength band. Let $N(\lambda_1, \lambda_2)$ represent the measured radiance in the region λ_1 to λ_2. For a blackbody,

$$N(\lambda_1, \lambda_2) = \int_{\lambda_1}^{\lambda_2} B(\lambda, T) d\lambda = \int_{\lambda_1}^{\lambda_2} \frac{2hc^2}{\lambda^5} \frac{d\lambda}{\exp[hc/(kT\lambda)] - 1} . \tag{3}$$

For any radiance measured within a specified wavelength window, there is an associated temperature such that at that temperature a blackbody would emit the same radiation. This is called the *brightness* temperature. All other things being equal, if we know the emissivity of a body and measure the emitted radiance, we can determine the body's true surface temperature.

There are three major limitations to using radiance measurements from an orbiting platform to estimate the sea surface temperature. First, clouds block infrared radiation from the surface. If cloudy regions are not appropriately identified, measurements of cloud temperature are incorrectly associated with sea surface temperature. Second, the intervening atmosphere absorbs some of the radiation emitted by the surface and it also emits radiation some of which goes directly to the satellite radiance sensor and some of which is reflected from the surface back up to the satellite. Third, solar radiation is reflected from the surface to the sensor. These problems are circumvented by procedures which identify cloudy regions or regions that may be contaminated with solar radiation. In addition, the effects of the intervening atmosphere are wavelength dependent. The passive measurement of radiation at different wavelengths can be used to infer an atmospheric correction.

Figure 1 shows the blackbody spectrum for an object at 300 K, roughly the spectrum of radiance from an ocean at the same temperature. The figure also shows the approximate spectrum of solar radiation reflected from the sea surface [2]. Reflected solar radiation from the surface is about 1% in the incoming solar radiation. The shaded regions indicate the wavelength bands used to measure radiance (channels 1–5) by the AVHRR.

Table 1 is a listing of AVHRR wavelength channels. Channels 1 and 2 measure reflected light in the visible and near infrared regions, respectively. Channels 3, 4, and 5 are dominated by radiation emitted from the surface. Channel 3 has the advantage that it is less sensitive to atmospheric water vapor. However, channel 3 will admit a substantial amount of reflected solar radiation. It is, therefore, primarily used at night. Channels 4 and 5 are more affected by water vapor, but are not
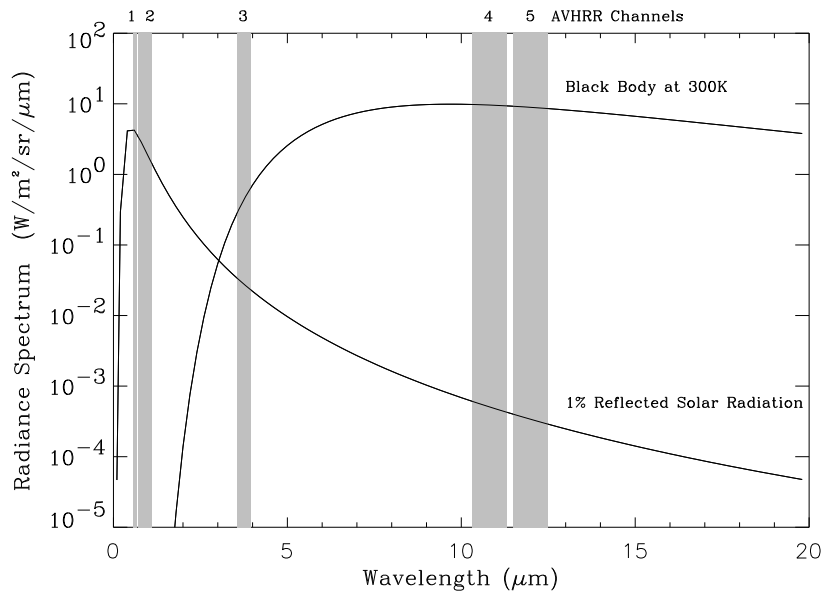
Figure 1: Blackbody radiation spectrum, reflected radiation spectrum and the wavelength channels used by the AVHRR sensor. Channels 1 and 2 are close in wavelength.

Table 1: Table of AVHRR channels.

Channel	Region	Wavelengths
1	Visible	0.58–0.68 μm
2	Reflected Infrared	0.725–1.1 μm
3	Emitted Infrared Window Channel	3.55–3.93 μm
4	Emitted Infrared Window Channel	10.33–11.3 μm
5	Emitted Infrared Window Channel	11.5–12.5 μm

substantially contaminated by reflected solar radiation. It is the judicious combination of radiance measurements from channels 3, 4 and 5 that permits extraction of sea surface temperature.

2.3 Sea Surface Temperature Algorithms

In Appendix A, we show why it is reasonable to believe that for nadir measurements in cloudless regions the sea surface temperature, T_s, should be of the form

$$T_s = a_0 T_i + a_1 (T_i - T_j) + a_2 \tag{4}$$

where T_i and T_j are the brightness temperatures determined from the radiance values in two different infrared window channels i and j. The constant a_0 is close to 1 suggesting that the infrared temperature measured in any one of these channels is close to the sea surface temperature. The temperature difference term makes a small correction to this temperature for atmospheric transmittance. The a_2 term is a small correction factor associated with the different atmospheric brightness temperatures at different channels.

Based on empirical comparisons of AVHRR data and buoy measurements, McClain *et al.* [3] and Bernstein [4] found two sets of algorithms for combining the radiance measurements at the three emitted infrared window channels — one set for nighttime and one set for daytime. The algorithms used at night can employ the $T_{3.7}$ channel. For daytime algorithms, the $T_{3.7}$ channel contains reflected skylight and only combinations of T_{11} and T_{12} are useful.

In general there are three classes of sea surface temperature algorithms. The "split-window" algorithm uses the T_{11} brightness temperature as the lowest order estimate of sea surface temperature and the difference $T_{11} - T_{12}$ to correct for the atmosphere. The "dual-window" algorithm uses the T_{11} brightness and the difference $T_{3.7} - T_{11}$ to correct for the atmosphere. Finally, the the "triple-window" algorithm uses the T_{11} brightness and the difference $T_{3.7} - T_{12}$ to correct for the atmosphere.

In addition, there are correction terms that must be applied to adjust the measurements made off nadir. If we define θ to be the sensor zenith angle, then the three algorithms have the form:

$$\text{Split (mc),} \quad T_s = A_0 T_{11} + A_1 (T_{11} - T_{12}) + A_2 (T_{11} - T_{12})(\sec\theta - 1) + A_3 \sec\theta + A_4$$

$$\text{Dual (bz),} \quad T_s = A_0 T_{11} + A_1 (T_{3.7} - T_{11}) + A_2 (T_{3.7} - T_{11})(\sec\theta - 1) + A_3 \sec\theta + A_4 \tag{5}$$

$$\text{Triple (tw),} \quad T_s = A_0 T_{11} + A_1 (T_{3.7} - T_{12}) + A_2 (T_{3.7} - T_{12})(\sec\theta - 1) + A_3 \sec\theta + A_4$$

The temperatures can either be in degrees Celsius or Kelvin. In Appendix B, we list the coefficients employed by the TeraScan software to compute sea surface temperature given these functional forms using both the Celsius and Kelvin temperature scales .

3 The TeraScan Procedures as Employed at APL

3.1 Storing Data

On the APL workstation *pauli* incoming AVHRR data is stored directly on disk. Four passes can be saved on disk at one time. As received, data are automatically archived to DAT (Digital Audio

Tape). New pass data replace older pass data on the computer disk.

The command `lspass` lists the data currently on disk. An example of the usage of the command is:

```
pauli: lspass
 #  satel    telem     date    day     time      durat   lines

 1  noaa-12  hrpt    95/12/12 346  12:19:21  10:45    3870
 2  noaa-12  hrpt    95/12/12 346  13:56:45  12:37    4543
 3  noaa-14  hrpt    95/12/12 346  17:35:41  15:14    5485
 4  unknown  hrpt    95/12/12 346  20:32:25  00:00       0
```

Each line represent a $\pm 55.4°$ scan of data sampled at increments of 1.3×10^{-3} radians.

The data on tape can be listed and retrieved using the `archive` command. All DAT tape operations are performed using this command. For example, here is a session where the DAT tape is rewound:

```
pauli: archive
operation        : char(  8) ? rewind
dev_name         : char(255) ? [/dev/rmt/0mn]
```

Note that the default tape device file is `/dev/rmt/0mn`.

An example of a session where the `archive` command is used to provide a listing of the data on DAT is shown below:

```
pauli: archive
operation        : char(  8) ? list
dev_name         : char(255) ? [/dev/rmt/0mn]
printout         : char(  3) ? [no]
catalog_pass     : char(  3) ? [no]
pass  satel    telem    date      time      orbit     scans     label
1     noaa-14  hrpt     95/12/12  06:09:50  0         5254      tape7
2     noaa-14  hrpt     95/12/12  07:50:17  0         5379      tape7
3     noaa-14  hrpt     95/12/12  09:32:58  0         3215      tape7
4     noaa-12  hrpt     95/12/12  10:37:44  0         3255      tape7
5     noaa-12  hrpt     95/12/12  12:19:21  0         3870      tape7
6     noaa-12  hrpt     95/12/12  13:56:45  0         4543      tape7
7     noaa-14  hrpt     95/12/12  17:35:41  0         5485      tape7
8     LASTPASS LASTPASS LASTPASS  LASTPASS  LASTPASS LASTPASS tape7
```

Tapes are initialized by choosing `init` as the option for the `archive` command. During the initialization, the user selects a tape label. We have been sequentially naming the tapes as `tape1`, `tape2,...`

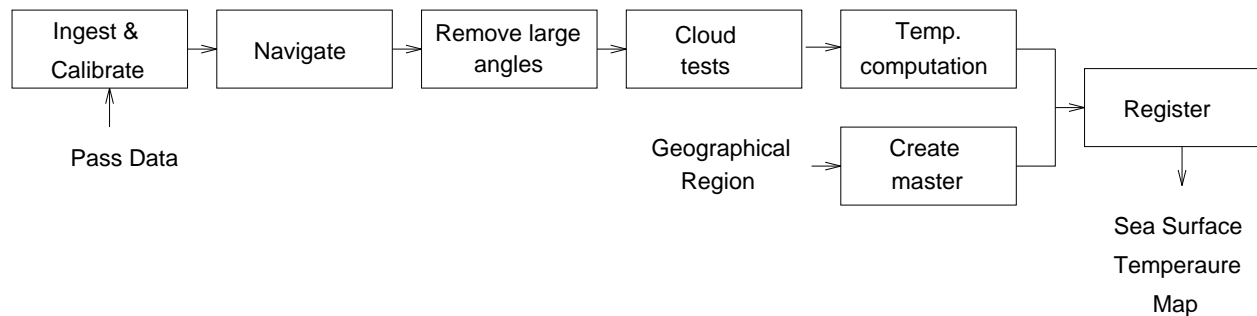## Sea Surface Temperature Processing Sequence

Figure 2: Sea surface temperature estimation procedure.

3.2 Data Ingestion

The steps necessary to produce sea surface temperature data from raw pass data are shown in Figure 2. In principle, the steps need not follow in exactly this order. Here, we show the sequence that has worked for us.

In order to perform any subsequent quantitative processing on the raw pass data, it is necessary to *ingest* a pass file using the TeraScan program `hrptin`. This puts the data into a special TeraScan format. If the calibration option if specified, the data are calibrated. Channels 1 and 2 are output in percent albedo using pre-launch calibration values specified in the `avcal.coef` file. Using measurements of deep space ($\sim$3 K) and internal blackbodies, whose temperature is measured with precision thermistors ($\sim$300 K), data in channels 3, 4, and 5 are calibrated and output in terms of brightness temperature. There is the option to output the data in units of Celsius, Kelvin or Fahrenheit.

Files generated by `hrptin` containing AVHRR have a `.avhrr` filename extension, by default.

3.3 Navigation

The next step is to navigate the data onto ground coordinates. The gross navigation is based upon Keplerian elements that are downloaded from SeaSpace daily. One may get the file `elements.new` from SeaSpace by using `ftp`. The address is `califia.seaspace.com`. The user name is `elements` and the password is `orbital3`. The command `fixoes` processes this data so that TeraScan software will use the new ephemeris elements.

More precise navigation can be performed automatically. The `navboxes` command used AVHRR data stored in `*.avhrr` files to generate a file, with a user selected name, which contains as set of boxes around coastlines for navigation.

The command `navigate` searches for cloud-free regions in the *.avhrr file and correlates the scene with know land boundaries to perform the fine-scale navigation. The correlation is performed in the boxes previously generated If sufficient cloud-free areas are available the image can be navigated to about a few kilometers. The data may also be navigated manually using the
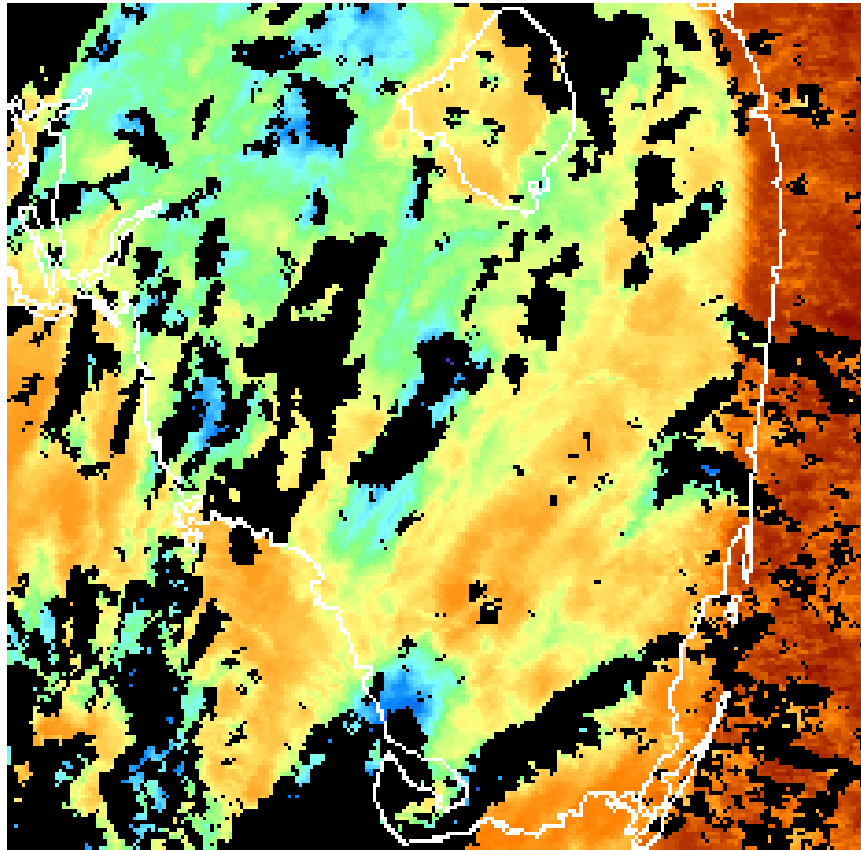
Figure 3: Example of sea surface temperature map with only ephemeris navigation.

`image/navigate` option from the interactive `xvu` program.

Figure 3 is sea surface temperature map in the south Florida area. The coastlines are placed on the image using only ephemeris information for navigation.

Figure 4 is also sea surface temperature map in the south Florida area. For this case the coastlines are placed on the image using ephemeris information and the `navigate` fine-scale autocorrelation program for navigation. Note that there has been significant improvement. It would be possible to manually improve the correspondence of the coastline data and the imagery.

3.4   Estimating Sea Surface Temperature

The next step is to take this temperature data and convert it to estimates of sea surface temperature. The `nitpix` command performs the necessary operations. The process involves first excluding data taken at large nadir angles. Next, image pixels contaminated with clouds are identified. Finally, a selected sea surface temperature algorithm is applied to the cloud-free pixels.

3.4.1   Exclusion of Data at Large Zenith Angles

Experience has shown that the sea surface temperature retrievals degrade as the sensor zenith angles increases — as we look further from nadir. The first step in the sea surface temperature
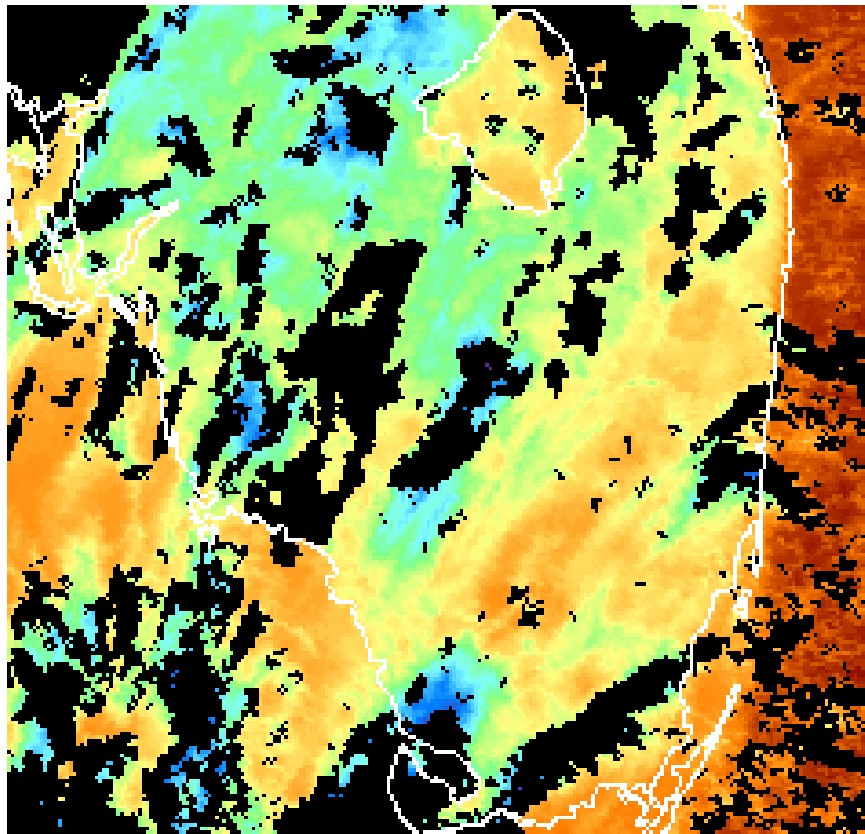
Figure 4: Example of sea surface temperature map with ephemeris and fine-scale navigation.

retrieval is to exclude pixels that are far from nadir. By default, TeraScan software excludes data beyond 53° from nadir.

3.4.2   Finding Cloud-Free Pixels

The sequence of steps to identify cloud involves several filters. Each pixel must satisfy all of the criteria to be judged cloud-free.

Channel 4 Difference.   The presence of sub-pixels clouds can change the apparent brightness temperature. If we assume that the sea surface temperature is slowly varying, then a large variance in a local region may indicate the presence of clouds. In the first cloud test, a 3×3 region around the pixel under consideration is used. If the difference between the maximum and minimum values within the 3×3 region is above a selected value, the center pixel is flagged as cloud contaminated. SeaSpace recommends this cutoff difference should be 2.5° and 1°, for daytime and nighttime, respectively.

Maximum Value in the Channel 2 Albedo.   A large albedo in channel 2 can indicate the presence of clouds. If the albedo of a pixel exceeds 8% for day or 2% for night, then the pixel is flagged as cloud contaminated.

Channel 2 Difference.   A large local variation in the albedo in channel 2 also indicates clouds. If the difference between the maximum and minimum albedo exceeds 2% in a 3×3 region around the pixel under consideration, the center pixel is assumed to contain clouds. This test is not used for daytime data.

Difference in Channel 3 and 4.   Channel 3 and channel 4 absorb significantly different proportions of water vapor. A large difference in the brightness temperatures in these two channels is an indication of cloud contamination. Since channel 3 may contain reflected sunlight, this test is used only at night.

Minimum Channel 4 Temperature.   If the channel 4 temperature is too low, we assume that we are seeing cloud-top temperatures. We have have not been using this as a strict cloud-elimination test. We accept all temperatures above 0°C.

Sea Surface Temperature Computation   The sea surface temperature algorithm has the form:

$$T_{\mathrm{s}} = A_0 T_{11} + A_1 (T_i - T_j) + A_2 (T_i - T_j)(\sec\theta - 1) + A_3 \sec\theta + A_4 \,, \tag{6}$$

i.e., sea surface temperature is the brightness temperature at 11 μm plus correction terms based on differences in brightness temperatures in different wavelength bands. The noise in the difference temperature is the root-mean-square sum of the individual temperature noise levels. To minimize this noise problem, the mean of the T_i and T_j within the 3×3 region around the pixel is used to compute the temperature difference.

    We provide an example of a `nitpix` session below:

Table 2: Preferred selections of the `nitpix` parameters.

Parameter	Default	Day	Night
cos_sat_zen	0.6	0.4	0.4
ch4_delta	0.3	2.5	1
ch2_max	3	8	2
ch2_delta	0.25	2	—
ch3_minus_ch4	0	0	−1.5
base_temp	0	0	0
temp_step	0.1	0.2	0.2
min_ch4_temp	0	0	0

```
pauli: nitpix
in/out files    : char(255) ? n14.95347.1905.avhrr n14.95347.1905.sst
sst_method      : char(  2) ? [mc]
cos_sat_zen     : real       ? [0.6] 0.4
ch4_delta       : real       ? [0.3] 2.5
ch2_max         : real       ? [3] 8
ch2_delta       : real       ? [0.25] 2
ch3_minus_ch4   : real       ? [0] 0
base_temp       : real       ? [0] 0
temp_step       : real       ? [0.1] 0.2
min_ch4_temp    : real       ? [0]
min_sun_reflect : real       ? [0]
mc noaa-14 D 1.017342 2.139588 0.779706 0.000000 -0.543000
```

For this session, the input file is `n14.95347.1905.avhrr`. This file was produced by the `hrtpin` program. The output sea surface temperature is written in file `n14.95347.1905.sst`. The second prompt indicates that the multi-channel (split-window) algorithm is used. The dual-window and triple-window algorithms are selected by answering `bz` and `tw`, respectively.

The `cos_sat_zen` parameter is the cosine the the maximum zenith angle. If 0.6 is selected then angles greater than $\cos^{-1}(0.6) = 53.1°$ from zenith are excluded. Here, we used 0.4 to avoid excluding any data.

The `ch4_delta`, `ch2_max`, `ch2_delta`, `ch3_minus_ch4` and `min_ch4_temp` are set in accordance with our previous discussion.

The `base_temp` and `temp_step` parameters control the scaling of the data.

The parameter `min_sun_reflect` is the minimum allowable angle (in degrees) between the reflected sun glint and the sensor look angle.

Table 2 lists preferred choices for the `nitpix` parameters for day and nighttime.

The final line output from `nitpix` is

```
mc noaa-14 D 1.017342 2.139588 0.779706 0.000000 -0.543000
```

This indicates that the daytime split-window algorithm for NOAA-14 is being used. The numerical coefficients for the sea surface temperature algorithm are listed.

By default, `nitpix` determines from the data whether to use the daytime or nighttime algorithms.

3.5 Create Images in a Defined Region

It is possible to define particular regions of interest using the `master2` program. This program creates a `Master` file with sufficient information so that any pass can be mapped into the defined area with a defined projection. Raw data are in satellite coordinates, each scan line is another increment along the satellite ground track. Each sample within a scan line is another increment of 1.3×10^{-3} r.

Consider the following example:

```
pauli: master2
output file    : char(255) ? [Master]
projection     : char( 13) ? rect
min_lat        : char( 15) ? 30n
max_lat        : char( 15) ? 50n
min_lon        : char( 15) ? 75w
max_lon        : char( 15) ? 60w
square_aspect  : char(  3) ? [yes]
num_samples    : int       ? 1000
est_center     : char(  3) ? [yes]
master2: 1741 lines, 1000 samples, 1.28042 km pixel height,
1.28042 km pixel width
```

This session creates a file called `Master` with the information necessary to map future passes into the geographical region from 30°N to 50°N and 75°W to 60°W. Images created using this `Master` file will have a rectangular projection and each pixel will have a square aspect ratio. The image will have 1000 samples per line and 1741 lines. Each pixel will represent a 1.28042 km × 1.28042 km area on the surface.

3.6 Create Registered Image

The final step is to use the `Master` file to create a registered sea surface temperature image in a specified coordinate system. The program to perform this registration is called `fastreg`. Below is a sample session.

```
pauli: fastreg
in/out files   : char(255) ? n12.95349.1250.sst n12.95349.1250.sst.fl
master_file    : char(255) ? [Master] /d10/noaa/masters/fl
include_vars   : char(255) ? []
poly_size      : real      ? [100]
n12.95349.1250.sst2.fl: mcsst: [   1,  740] X [   1,  790]
```

In this session, `fastreg` takes the sea surface temperature file `n12.95349.1250.sst` uses a master file `/d10/noaa/masters/fl` to produce a ground registered image named `n12.95349.1250.sst.fl`.

4   Conclusion

In this memorandum, we have reviewed the physics behind sea surface temperature measurements using downlinked AVHRR data from the NOAA satellites. We have also described the procedures necessary to process data using the TeraScan software. Ray Sterner, who mastered much of the TeraScan software and has provided advice on sea surface temperature processing, in currently completing batch software which should permit the automatic processing of the incoming NOAA data. The goal is to archive all data and to produce synoptic scale images for post-processing browsing.

Appendicies

A Justification for the Functional Form of the Sea Surface Temperature Algorithm

Let $N(T)$ represent the blackbody radiance at temperature T in a specified wavelength regime. The radiance measured at a satellite is the sum of the ocean radiance, plus radiance emitted from the atmosphere, plus the sky radiance reflected from the surface. See Figure A-1. This can be expressed as

$$\overbrace{N_m(T_m)}^{\text{Measured}} = \overbrace{\tau_a\varepsilon_w N(T_s)}^{\text{Ocean}} + \overbrace{\varepsilon_a N(T_a)}^{\text{Atmosphere}} + \overbrace{\tau_a r_w N_{sky}}^{\text{Reflected Sky Radiance}} \tag{A-1}$$
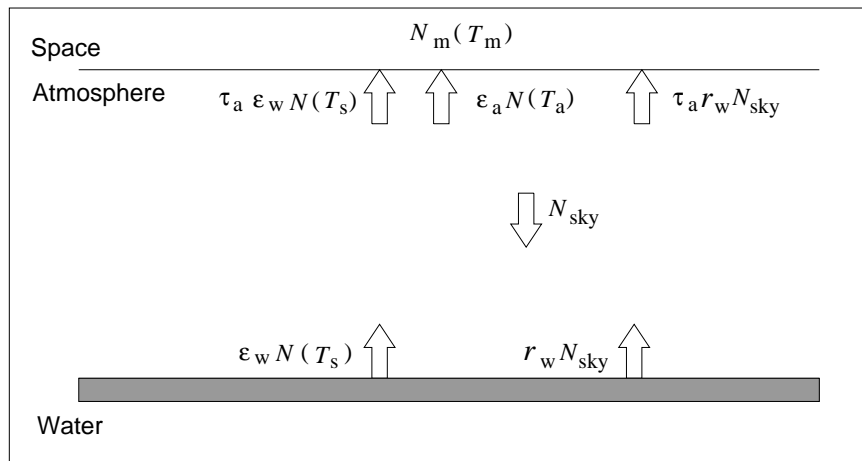
Figure A-1: Measured radiances.

where

N_m radiance measured at the satellite,

τ_a is the transmittance of the atmosphere,

ε_w is the emissivity of water,

$N(T_s)$ is the blackbody radiance at the sea surface temperature of T_s,

r_w is the reflectivity of water, and

N_{sky} is the downwelling sky radiance,

We know that atmospheric emissivity, ε_a, equals $1 - \tau_a$ and that the emissivity of water, ε_w equals $1 - r_w$. We substitute these relations in Equation A-1 and we get

$$N_m(T_m) = \tau_a(1 - r_w)N(T_s) + (1 - \tau_a)N(T_a) + \tau_a r_w N_{sky} . \tag{A-2}$$

Rearranging terms yields

$$N_m(T_m) = \tau_a N(T_s) - r_w \tau_a N(T_s) + N(T_a) - \tau_a N(T_a) + \tau_a r_w N_{sky} \qquad (A\text{-}3)$$

or

$$N_m(T_m) = \tau_a N(T_s) - \overbrace{r_w \tau_a N(T_s)\left[1 - \frac{N_{sky}}{N(T_s)}\right]}^{\text{small}} + (1 - \tau_a)N(T_a) . \qquad (A\text{-}4)$$

Since the reflection coefficient of water is small, we eliminate the middle term on the right-hand side of the previous equation and get

$$N_m(T_m) = \tau_a N(T_s) + (1 - \tau_a)N(T_a) . \qquad (A\text{-}5)$$

We now perform a Taylor's series expansion for $N_m(T_m)$ about the sea surface temperature, keeping the first two terms. We rewrite $N_m(T_m)$ as

$$N_m(T_m) = N(T_s) + \frac{\partial N(T_s)}{\partial T}(T_m - T_s) \qquad (A\text{-}6)$$

Substitute this relation into the left-hand side of Equation A-5. The resulting equation is

$$N(T_s) + \frac{\partial N(T_s)}{\partial T}(T_m - T_s) = \tau_a N(T_s) + (1 - \tau_a)N(T_a) . \qquad (A\text{-}7)$$

We may also expand $N(T_a)$ as

$$N(T_a) = N(T_s) + \frac{\partial N(T_s)}{\partial T}(T_a - T_s) . \qquad (A\text{-}8)$$

Substitution of this into Equation A-7 yields

$$N(T_s) + \frac{\partial N(T_s)}{\partial T}(T_m - T_s) = \tau_a N(T_s) + (1 - \tau_a)\left[N(T_s) + \frac{\partial N(T_s)}{\partial T}(T_a - T_s)\right] . \qquad (A\text{-}9)$$

By eliminating like terms in the previous equation and dividing by $\partial N(T_s)/\partial T$ we get

$$T_m = \tau_a T_s + (1 - \tau_a)T_a \qquad (A\text{-}10)$$

Equation A-10 is valid at two channels i and j and we can rewrite Equation A-10 for two wavelengths as

$$T_i = \tau_{a_i} T_s + (1 - \tau_{a_i})T_{a_i} \qquad (A\text{-}11)$$

and

$$T_j = \tau_{a_j} T_s + (1 - \tau_{a_j})T_{a_j} . \qquad (A\text{-}12)$$

The difference $T_i - T_j$ is then given as

$$T_i - T_j = T_s(\tau_{a_i} - \tau_{a_j}) + (1 - \tau_{a_i})T_{a_i} - (1 - \tau_{a_j})T_{a_j} \qquad (A\text{-}13)$$

By multiplying Equation A-11 by τ_{a_j} and Equation A-12 by τ_{a_i}, we generated the following two equations:

$$\tau_{a_j}T_i = \tau_{a_i}\tau_{a_j}T_s + (1 - \tau_{a_i})T_{a_i} \tag{A-14}$$

$$\tau_{a_i}T_j = \tau_{a_i}\tau_{a_j}T_s + (1 - \tau_{a_j})T_{a_j} \tag{A-15}$$

We now subtract Equation A-15 from Equation A-14, yielding

$$\tau_{a_j}T_i - \tau_{a_i}T_j = \tau_{a_j}(1 - \tau_{a_i})T_{a_i} - \tau_{a_i}(1 - \tau_{a_j})T_{a_j} \tag{A-16}$$

Subtracting Equation A-16 from Equation A-13, we write:

$$\begin{aligned}
T_i(1 - \tau_{a_j}) - T_j(1 - \tau_{a_i}) = \\
T_s(\tau_{a_i} - \tau_{a_j}) + \left[(1 - \tau_{a_i}) - \tau_{a_j}((1 - \tau_{a_i})\right]T_{a_i} - \left[(1 - \tau_{a_j}) - \tau_{a_i}(1 - \tau_{a_j})\right]T_{a_j} = \\
T_s(\tau_{a_i} - \tau_{a_j} + (1 - \tau_{a_i})(1 - \tau_{a_j})T_{a_i} - (1 - \tau_{a_j})(1 - \tau_{a_i})T_{a_j} .
\end{aligned} \tag{A-17}$$

Solving for T_s we obtain

$$T_s = T_i + \frac{1 - \tau_{a_i}}{\tau_{a_i} - \tau_{a_i}}(T_i - T_j) - \frac{(1 - \tau_{a_i})(1 - \tau_{a_j})}{\tau_{a_i} - \tau_{a_i}}(T_{a_i} - T_{a_j}) \tag{A-18}$$

We conclude that the absence of clouds and observations at nadir, sea surface temperature may be written as

$$T_s = a_0 T_i + a_1(T_i - T_j) + a_2 . \tag{A-19}$$

For the approximations used here, $a_0 \sim 1$, *i.e.,* at the lowest order the sea surface temperature equals the measured brightness temperature. The parameter $a_1(T_i - T_j)$ accounts for the atmospheric transmittance. The last term is a small correction associated with the different brightness temperatures of the atmosphere at the two measurement wavelengths.

B   Coefficients for Sea Surface Temperature Algorithms

setcountertable0

Tables B-1, B-2 and B-3 list the parameters the TeraScan software uses to compute sea surface temperature for the split-window, dual-window and triple-window algorithms, respectively. Coefficients are valid for temperatures in both Kelvin and Celsius. The only exception is that the term A_4 varies depending upon the temperature scale.

Table B-1: Coefficients for split-window algorithm.

Satellite	Time	A_0	A_1	A_2	A_3	A_4(K)	A_4(C)
noaa-14	D	1.017342	2.139588	0.779706	0.000	-5.280	-0.543
noaa-14	N	1.029088	2.275385	0.752567	0.000	-9.090	-1.145
noaa-12	D	1.013674	2.443474	0.314312	0.0	-4.647	-0.912
noaa-12	N	1.013674	2.443474	0.314312	0.0	-4.647	-0.912
noaa-11	D	1.01345	2.659762	0.526548	0.0	-4.592	-0.918
noaa-11	N	1.052	2.397089	0.959766	0.0	-15.52	-1.316
noaa-9	D	0.9994	2.7057	-0.27	0.73	0.1177	-0.046
noaa-9	N	0.9994	2.7057	-0.27	0.73	0.1177	-0.046
noaa-7	D	1.0346	2.5779	0.0	0.0	-10.05	-0.60
noaa-7	N	1.0346	2.5779	0.0	0.0	-10.05	-0.60
noaa-10	D	1.1	0.0	0.0	0.0	-27.316	0.0
noaa-10	N	1.1	0.0	0.0	0.0	-27.316	0.0
noaa-8	D	1.1	0.0	0.0	0.0	-27.316	0.0
noaa-8	N	1.1	0.0	0.0	0.0	-27.316	0.0
noaa-6	D	1.1	0.0	0.0	0.0	-27.316	0.0
noaa-6	N	1.1	0.0	0.0	0.0	-27.316	0.0

Table B-2: Coefficients for dual-window algorithm.

Satellite	Time	A_0	A_1	A_2	A_3	$A_4(K)$	A_4(c)
noaa-14	N	1.008751	1.409936	0.000000	1.976	-0.764	1.626
noaa-12	D	1.017736	0.426593	1.800916	0.0	-3.114	1.731
noaa-12	N	1.017736	0.426593	1.800916	0.0	-3.114	1.731
noaa-11	D	1.03432	1.347423	0.953042	0.0	-7.64	1.73
noaa-11	N	1.03432	1.347423	0.953042	0.0	-7.64	1.73
noaa-9	D	1.014	0.5118	0.958	1.55	-2.224	1.60
noaa-9	N	1.014	0.5118	0.958	1.55	-2.224	1.60
noaa-10	D	1.009	1.502	0.0	-1.2	-2.58	-0.12
noaa-10	N	1.009	1.502	0.0	-1.2	-2.58	-0.12
noaa-8	D	1.009	1.502	0.0	-1.2	-2.58	-0.12
noaa-8	N	1.009	1.502	0.0	-1.2	-2.58	-0.12
noaa-7	D	1.009	1.502	0.0	-1.2	-2.58	-0.12
noaa-7	N	1.009	1.502	0.0	-1.2	-2.58	-0.12
noaa-6	D	1.009	1.502	0.0	-1.2	-2.58	-0.12
noaa-6	N	1.009	1.502	0.0	-1.2	-2.58	-0.12

Table B-3: Coefficients for triple-window algorithm.

Satellite	Time	A_0	A_1	A_2	A_3	A_4(K)	A_4(C)
noaa-14	N	1.010037	0.920822	0.000000	1.760	2.214	0.528
noaa-12	N	1.058532	1.016347	0.0	2.081917	-3.407	12.58
noaa-11	N	1.036027	0.892857	0.520056	0.0	-9.224	0.617

References

[1] Eisberg, R. M., *Fundamentals of Modern Physics*, John Wiley and Sons, New York, NY, 47–69, 1961.

[2] Stewart, R. H., *Methods of Satellite Oceanography*, University of California Press, Berkley, CA, 128–152, 1985

[3] McClain, E. P., W. G. Pichel, and C. C. Walton, "Comparative performance of AVHRR-based multichannel sea surface temperature," *J. Geophys. Res., 90,* 11,587–11,601, 1985.

[4] Bernstein, R. L., "Sea surface temperature estimation using the NOAA-6 advanced very high resolution radiometer", *J. Geophys. Res., 87,* 9455– 9465, 1982.